4. Preclinical evaluation of DNA nanoparticles for ophthalmic drug delivery

4.1 Introduction

Treatment of eye diseases is accompanied with many problems. Therefore, improvement in efficacy of eye drops has been an important goal for many years. By increasing the duration time of the medication a lower regime can be attained, resulting in an improved compliance. In addition, it allows for a lower drug concentration, what results in fewer side effects and therefore gives the possibility to use medication that is currently harmful to apply.

In the past, the effectiveness of eye drops has been slightly increased by changing the viscosity and composition of the drops. Examples are formulations containing hyaluronic acid[1-2] or a carbomer solution composed of several lipids[3]. However, this resulted in very little improvement and causes reduced vision when the medicine is applied, which in turn leads to a lack of compliance. As such improvement of eye drops has been pursued through the use of different nanoparticles (NPs)[4-5]. Among several different systems, liposomes and micelles are the most popular ones due to the ease of fabrication and commercial availability of the building blocks. Micellar NPs are typically comprised of diblock copolymers that are biocompatible and

biodegradable. Commonly used polymers include poly(lactic acid)(PLA)[6], poly(lactic-*co*-glycolic acid) (PLGA)[7-8], poly(ethylene oxide)(PEO)[9] and poly(*N*-isopropylacrylamide) (polyNIPAAm)[10]. The other frequently used nanocarriers, liposomes, are composed of lipids that have a hydrophobic tail and hydrophilic headgroup. These species self-assemble into spherical structures exhibiting an aqueous inner environment enveloped by a lipid bilayer membrane. Especially nanosystems with a positive charge at the surface have proven to increase the bioavailability of several drugs due to their interaction with the corneal mucin layer that is negatively charged[11-13].

Although the above mentioned delivery systems have great advantages over pristine formulations, they also have several limitations. These particles are not uniform in size or composition and surface functionalization often is cumbersome. In this respect DNA based nanoparticles have several advantages. Due to the complete control over the number and spatial orientation of the functional groups these particles can very easily be tailored [14-15]. Despite these benefits, NPs composed of nucleic acids have not been used in the field of ophthalmology. Therefore, we investigated the use of DNA nanoparticles containing lipid-modified nucleotides for ocular drug delivery.

As with other nanoparticulate systems loading of medication can be performed through hydrophobic interactions or by covalent attachment to the carrier (See Fig 4.1). The former strategy, however, is limited to hydrophobic drugs, which excludes a large number of compounds such as most antibiotics. The latter method requires chemical modification of the drug which might impair with binding of the drug to the target and requires cleavage from the carrier. Therefore, we proposed a more elegant strategy that allows for specific loading without the need of alteration of the target molecule. This can be achieved through the use of aptamers[16] that are elongated with the complementary sequence and simply hybridized to the single stranded corona of the DNA NPs. This method enables the loading of virtually any molecule of interest as aptamers can reliably be developed

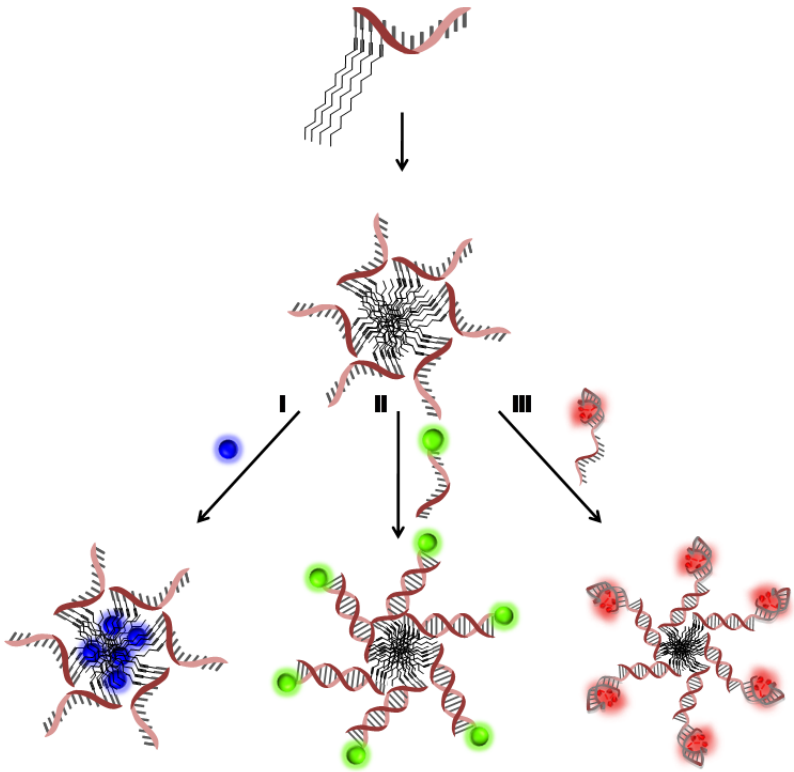

Figure 4.1. Schematic drawin of possible loading stratigies for DNA based NPs using hydrophobic interactions (I), covalent attachment to the complementary strand (II) or employing an extended aptamer seequence (III).

using systematic evolution of ligands by exponential enrichment (SELEX)[17-19]. In short, this process involves the exposure of a library of oligonucleotides to the immobilized target. After a washing step the binding sequences are eluted and amplified by the use of PCR. The amplified binders are then again exposed to the target and the procedure is repeated. Through multiple selection cycles and with more stringent washing conditions throughout the repetitions the strongest binding sequences are selected.

In this chapter, the translation from adherent NPs to true drug delivery vehicles is presented. To this end, the best adhering NP system developed in chapter 3 was loaded with two well-known antibiotics, i.e., neomycin B and kanamycin B. These are currently used in the clinic for treatment of ocular inflammation. To incorporate drug molecules, a DNA aptamer binding

kanamycin B[20] and a RNA aptamer binding neomycin B[21] were extended at the 3' end with the complementary sequence of the U4-12 DNA amphiphile. Watson-Crick base pairing of aminoglycoside-complexed aptamers and DNA nanoparticles resulted in two antibiotic-loaded nanocarrier systems (See Fig. 4.1, III), proving the general drug loading strategy. With one of the first *in-vivo* delivery examples of DNA nanotechnology we show that the long residence time of the nanoparticles can be translated into improved efficiency compared to the pristine drug, even demonstrating applicability with human tissue.

4.2 Results and discussion

4.2.1 Delivery of antibiotic-loaded NPs to the cornea

After completion of proof-of-concept experiments we investigated aptamer-functionalized U4-12 carriers loaded with neomycin B and kanamycin B. These two antibiotics are widely used for treatment of ocular infections and can be anchored to a DNA NP via well characterized high affinity aptamers[20-21]. To compare the time-dependent clearance of the antibiotic and the drug-loaded carrier they were administered *in-vivo* to rats. As control, the same antibiotics were labeled with a green fluorescent dye (fluorescein) at one of the amine groups. For imaging of the NPs the aptamer was functionalized with a red fluorescent dye (Cy3) at the 5' end. Eye drops of approximately 30 µl and containing equal amounts of either NP-bound antibiotic or free antibiotic were administered to live rats at a concentration of 20 µM and the adherence to the cornea was studied 5, 15, 30 minutes, 1, 2 and 4 hours after application (See Fig. 4.2).

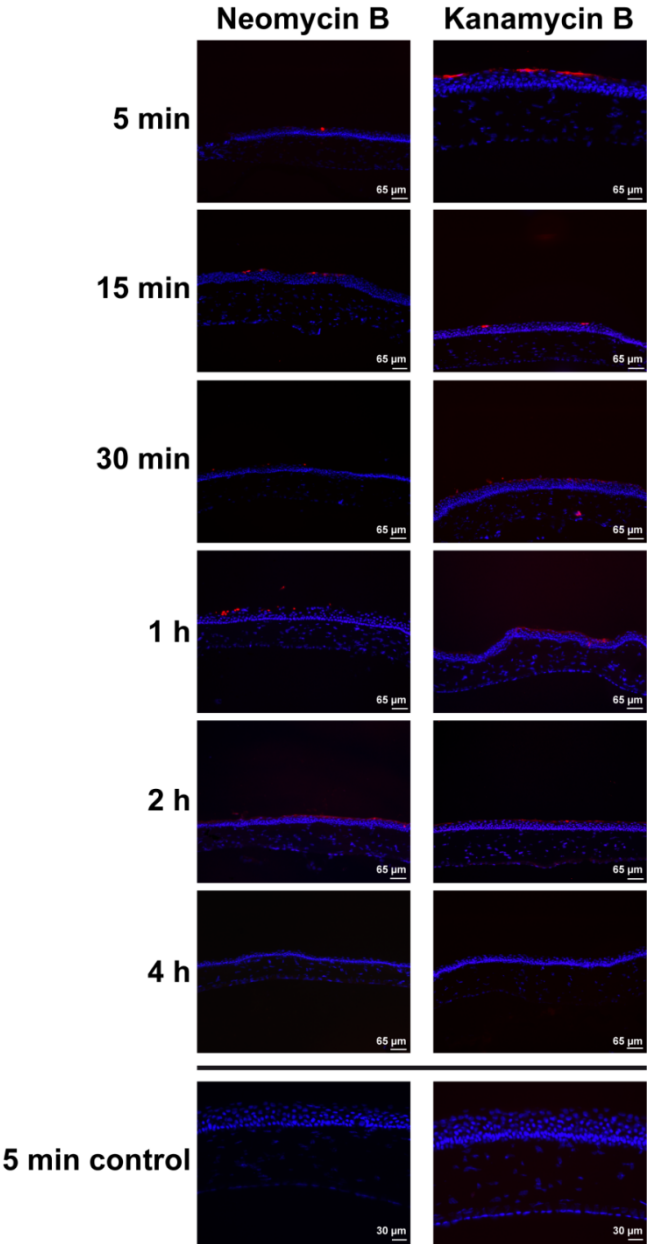

Figure 4.2. Fluorescence images demonstrating adhesion of neomycin B- (left) and kanamycin B-loaded (right) NPs (red) to the rat cornea (blue). In the images in the bottom row, a fluorescently labelled form of the free antibiotic was used as a control (green). The time point after administration of the antibiotic-loaded NP or free antibiotic is indicated on the left.

Both neomycin B- and kanamycin B-loaded NPs are effectively attached to the cornea for a period of at least 2 hours, whereas the fluorescent antibiotics are not detectable after only 5 min. These experiments indicate that adhesion to the cornea is greatly enhanced by the carrier system, which allows the loading of different cargoes and their close contact to the corneal surface. It is important to mention in this context that the chemical structure of the drugs was not modified due to the non-covalent nature of NP loading. Since RNA and DNA aptamers are known to bind a large variety of molecular structures[16-17] these vehicles represent a general delivery platform for diseases of the anterior section of the eye that can be loaded with drugs in a modular fashion.

4.2.2 Adherence of antibiotic loaded NPs to the human cornea

To demonstrate the translatability of this nanocarrier system from the rat model to humans, we examined the adherence of antibiotic-loaded particles to human corneal tissue. The experiments were performed on discarded tissue from corneal transplantations. Eye drops containing nanoparticles loaded with fluorescently labeled aptamers were administered to the corneal epithelium, the tissue was incubated for five minutes and afterwards the cornea was washed. Similar to previous experiments, fluorescently labeled antibiotics were used as control. Washing times after incubation were varied between five minutes and two hours (See Fig. 4.4). Both neomycin B- and kanamycin B-loaded NPs showed a remarkable attachment to the human cornea, while the free drugs were displaced at the first time point. A slow decrease in intensity was observed for increasing washing times for particles containing neomycin B. This can be due to detachment of the NPs from the corneal surface or because of degradation of the aptamer. In contrast, for kanamycin B this effect was not notable.

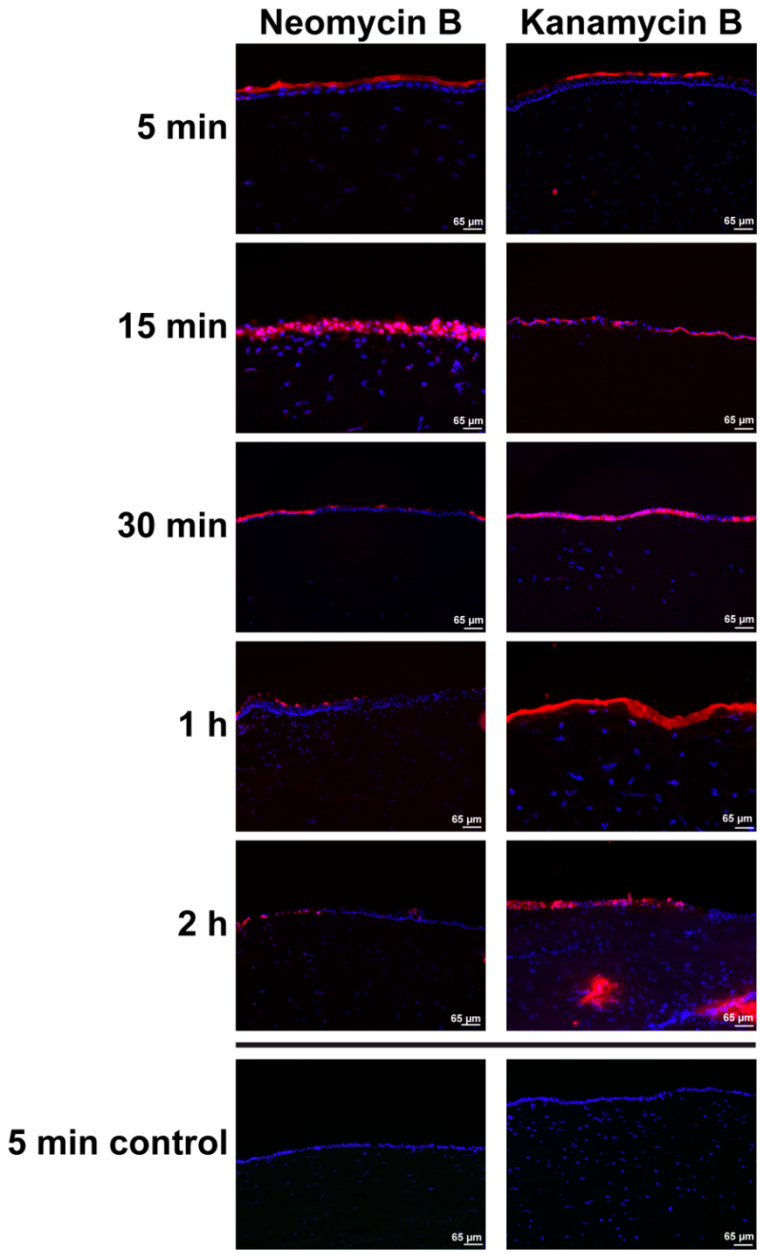

Figure 4.3. Adhesion of neomycin B- (left) and kanamycin B- (right) loaded NPs (red) to human cornea(blue), as monitored by fluorescence microscopy. After administration of the NP, the tissue was washed for the times indicated on the left. In the images in the far right column, a fluorescently labelled form of the free antibiotic was used as a control (green).

4.2.3 Antimicrobial activity of loaded NPs in medium

Next, we investigated whether an improved adherence half-life of the NPs translates into better activity and efficacy compared to the pristine drug. To do so, we first demonstrated that the antibiotic can be liberated from the NP by subjecting antibiotic-loaded NPs to a minimum inhibitory concentration test (MIC-test) using Escherichia coli (E. coli)(See Fig. 4.4). For this purpose, the action of antibiotic loaded NPs was compared to the free drugs. To mimic nuclease containing body fluids on the ocular surface, RNAse and DNAse were added to the cell suspension containing neomycin B- and kanamycin B-loaded NPs, respectively. The growth progress was determined by measuring the optical density of the cell suspension at 600 nm after 5 hours incubation at 37 °C

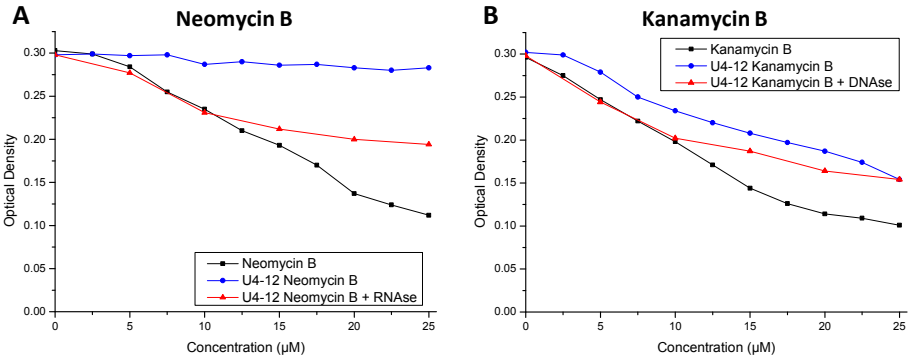

Figure 4.4. E. coli growth dependence on antibiotic concentration after 5 hours of incubation at 37°C with (A) neomycin B and (B) kanamycin B, for the free compound (black), the antibiotic loaded in the NP (blue) and the antibiotic loaded in the NP in the presence of DNA/RNAse (red).

The MIC tests clearly demonstrate that under *in-vivo*-like conditions, both nanocarrier-loaded antibiotics are active. As expected, for the free aminoglycosides a clear decrease in cell growth was observed with increasing antibiotic concentration. Neomycin B-loaded NPs, however, require the presence of RNAse to release the drug and induce bactericidal effects while the presence of DNAse has little impact on the effectiveness of

kanamycin B-loaded NPs. In the context of *in-vivo* applications, neither the RNAse-dependent release of the neomycin B nor the DNAse-independent release of the kanamycin B presents an obstacle because nucleases are prevalent in biological fluids[22].

4.2.4 Activity and Efficacy of antibiotic-loaded NPs

Having demonstrated that the NPs exhibit excellent adhesive properties on the cornea and that the antibiotic activity is retained in an *in-vivo*-like environment, in a next step we determined whether a clear antibiotic effect can be observed at the site of action. To this end, growth studies of E. coli were performed on porcine corneas where the efficacy of antibiotic-loaded NPs was compared to that of the free drugs. Growth inhibition was first evaluated without washing by incubating the cornea from porcine eyes with antibiotic-loaded NPs for 5 minutes. At the end of the incubation period, excess solution was removed and the corneas were placed on petrifilms containing growth medium. A total of on average 50 E.coli bacteria were applied to the cornea and were allowed to grow for 48 hours, after which the number of bacterial colonies was determined (See Fig. 4.5).

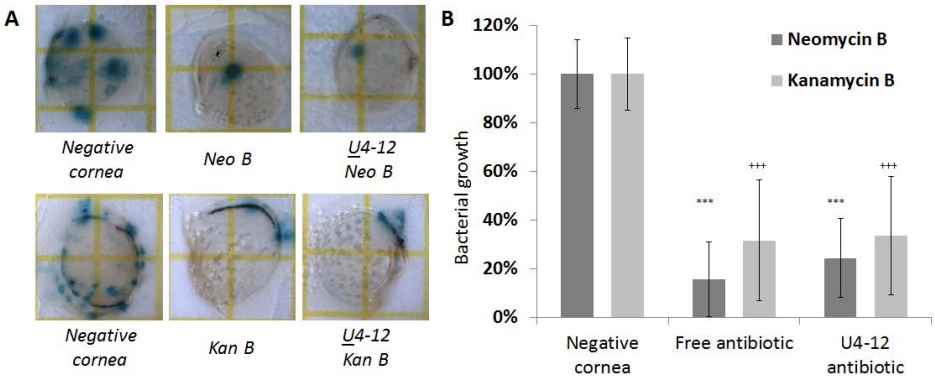

Figure 4.5. Bacterial growth experiments on porcine corneas treated with buffer (Negative cornea), free antibiotic and antibiotic-loaded NPs (U4-12) without washing. (A) Representative photographs of E. coli growth on unwashed porcine corneas. (B) Growth experiment without washing (n = 4-5). Control (Negative cornea) is set to 100% growth. Statistical differences are shown as * for neomycin B and +++ for kanamycin B, with p<0.001 compared to negative cornea. Comparison between the loaded U4-12 NPs and the free antibiotics did not show significant differences.**

The growth experiments clearly show the antibacterial activity after incubation of the cornea with free antibiotics. The antibiotics bound to the NPs show a similar growth inhibition, suggesting that the aptamers are degraded by nucleases or that the drugs are otherwise fully released from the NPs within the timeframe of the experiment.

After confirming the antibiotic activity on the cornea further growth experiments were performed where tearing was simulated by washing the porcine corneas with an excess of buffer to evaluate the efficacy of the kanamycin B-loaded NPs that are bound tightly to the cornea. Therefore, the same setup was utilized, but after incubation with the NPs the porcine cornea was washed with a large excess of PBS for 5, 30 and 60 minutes (See Fig. 4.6). The results of the E.coli growth experiment on corneas washed for 5, 30 and 60 minutes after exposure to kanamycin B-loaded NPs illustrate one of the shortcomings of current ophthalmic medication. No significant growth inhibition is found for the free antibiotic after 5 minutes of washing, indicating that the drug molecule is washed away within this short period of time. This is in good agreement with results from experiments where fluorescently labeled free antibiotics were not detected by fluorescence microscopy 5 minutes after application to the rat cornea *in-vivo* and the human cornea *in-vitro*. In contrast, the porcine corneas treated with the NPs containing kanamycin B exhibited bactericidal activity after up to 30 minutes of washing. Again, this is in good agreement with the extended NP adhesion time observed on the rat cornea. These experiments establish that the long adherence time of the NPs can be translated into a higher efficiency of the antibiotic treatment when employing the nanocarrier compared to the free drug.

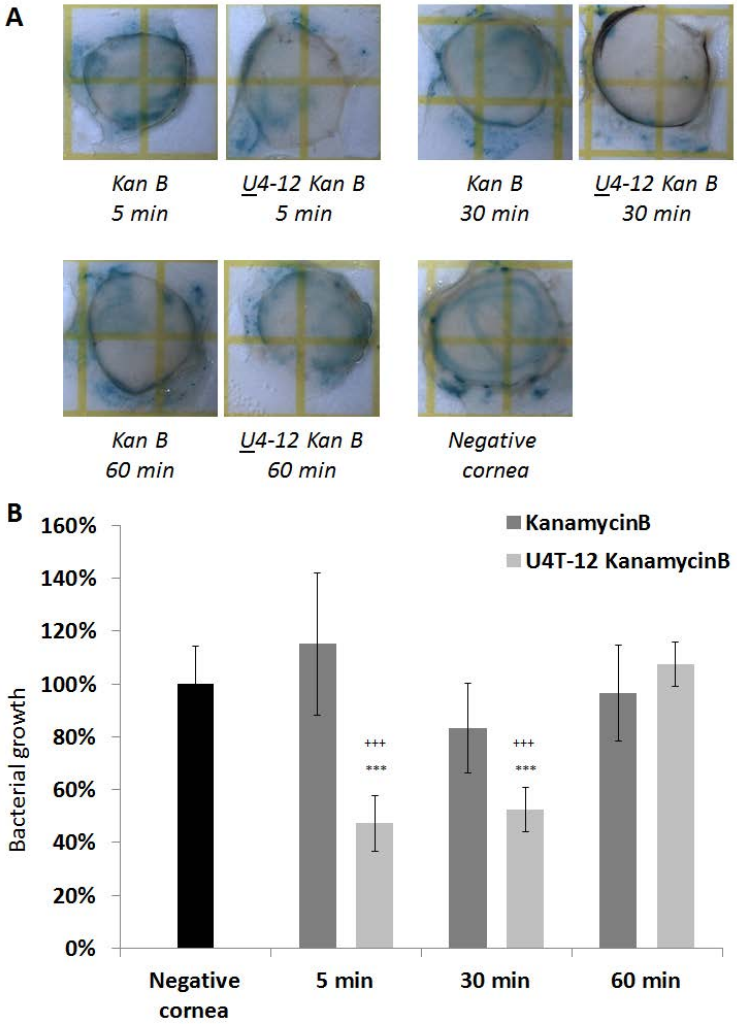

Figure 4.6. Bacterial growth experiments on porcine corneas treated with buffer (Negative cornea), free kanamycin B and kanamycin B-loaded NPs (U4-12) with washing. (A) Representative photographs of E. coli growth with varying washing times. (B) Growth experiment with varying washing times (n = 3-4). Control (Negative cornea) is set to 100% growth. Statistical differences are shown as * with p<0.001 compared to negative cornea. Comparison between kanamycin B and kanamycin B-loaded U4-12 NPs are shown as +++ with p<0.001. Unmarked time-points were not significantly different. Differences between the time-points were not evaluated.**

4.3 Conclusion

Treatment of eye diseases by eye drops is complicated by several means and improving efficacy of eye drops has been an important goal for many years[23]. By increasing the exposure time of the target tissue to the active compound in the drops, less frequent administration of less concentrated drops would be required. As a consequence, improved compliance is to be expected alongside lower levels of side effects, providing the opportunity to administer medication that is toxic at the concentrations currently required[24].

Here, we have shown a novel, powerful and general approach for treating eye infections using DNA nanotechnology that can be easily extended to treat other ocular indications. A paramount feature is the use of aptamers for drug loading, which enables specific binding of virtually any drug to the carrier without chemical modification or alteration of the pharmaceutical function. Because aptamers can be evolved against molecules with very diverse structures, this approach represents a truly modular drug delivery platform. We have demonstrated functionalization of the DNA carrier with therapeutically active agents, imaging units or a combination of the two by simple mixing of components and hybridization to generate multifunctional nanoobjects. The NPs have proven to dramatically increase the adherence time of antibiotics on the cornea in living animals and human tissue. Furthermore, antibiotic-loaded NPs have shown to be more effective than free antibiotics in preventing bacterial growth on porcine corneal tissue under conditions simulating tear fluid production, with an increased residence time at least 10-fold higher than the pristine drug. These findings open a variety of possibilities for utilization of DNA-based materials in ophthalmic drug delivery.

4.4 Experimental

4.4.1 Preparation of functionalized NPs

Antibiotic-loaded NPs were prepared at the needed concentration (20 µM) in 1x TAE buffer (40 mM Tris-Acetate, 1 mM EDTA, 20 mM NaCl, 12 mM MgCl2, pH 8.0). For loading of neomycin B and kanamycin B a RNA and DNA aptamer was used, respectively, both were elongated with the complementary sequence of the carrier (See Table 4.1). The lipid modified oligonucleotide U4-12 and the complementary DNA-aptamer (1 eq.) were loaded in a tube at the desired concentration and hybridized using a thermal gradient (80 °C, 30 min; 1°C/2 min until RT). When nanoparticles were used for fluorescent imaging a 5' Cy3 functionalized aptamer was used. Subsequently, for neomycin B two equivalents of antibiotic were added and for kanamycin B one equivalent (10 mM stock solution in ultrapure water). The solution was incubated at RT for a minimum of 30 minutes and used without further dilution.

Name	Sequence (5' → 3')
cU4-neo	GGACUGGGCGAGAAGUUUAGUCCGCGAAUCCGCAAAA
cU4-kan	TGGGGGTTGAGGCTAAGCCGATTGAATCCGCAAAA

Table 4.1. Sequence of extended aptamers used for antibiotic loading of NPs.

4.4.2 Adherence of antibiotic-loaded NPs to living rat eyes

The adherence of antibiotic-loaded NPs was determined as described in Chapter 3, section 3.4.5. In short, a single eye drop of approximately 30 µl of the NP containing solution was administered to the fixated rat. Blinking of the eyes was not hindered during drop application or afterwards. After the designated incubation time the rat was sacrificed with carbon dioxide inhalation. After sacrificing the animal, the eyes were enucleated and frozen in Tissue-Tek O.C.T. (Sakura Finetek, Germany) using liquid nitrogen. Frozen sections were longitudinally cut (12 µm) on a cryostat (Leica CM 1900, Germany), thaw-mounted onto glass slides (Superfrost plus, R. Langenbrinck Labor- und Medizintechnik, Germany) and stored at -30 °C until further use. For visualization, sections were fixed with methanol and to

stain nuclei sections were further incubated in a solution containing 0,2µg/ml 4`,6-diamidino-2-phenylindol (DAPI) for 1 min. Stained sections were embedded in FluorSave (Calbiochem, Germany) and imaged using a fluorescent microscope (Axioplan2 imaging®, Zeiss, Germany with Openlab software, Improvision, Germany)[25]. Animals were treated according to the principles of laboratory animal care (NIH publication No. 85-23, revised 1985), the OPRR Public Health Service Policy on the Human Care and Use of Laboratory Animals (revised 1986) and the German animal protection law (research permission AK3/11 to Sven Schnichels)

4.4.3 Human cornea experiments

Five human cornea rims were kindly provided by the eye bank of the University Eye Hospital Tübingen after approval of the planned experiments. These rims are leftover tissue after a corneal transplantation. Informed consent was obtained from all human subjects. After the transplantation the cornea rims were returned to the cornea media (KM1, Biochrom, Deutschland) until further use. Before applying the nanoparticles the corneas were cut into 3-4 equal sized pieces, transferred to a 24-well plate and washed with PBS (PAA, Germany). Afterwards, 100 µl of the nanoparticles were applied on top of the cornea and incubated at room temperature for the designated time. Then the corneas were transferred to another well containing 2 ml of PBS and washed for the designated time at room temperature. Next the corneas were frozen in Tissue Tek, cut on a cryostat, stained with DAPI and photographed as described previously.

4.4.4 Minimum inhibitory concentration tests

For inhibitory test Escherichia coli (E. coli), kindly donated by Sukirthini Balendran, Molecular Genetics Laboratory, Centre for Ophthalmology, Institute for Ophthalmic Research, Tübingen was grown in 1x LB medium (0.5% yeast extract, 1% tryptone, 1% NaCl) at 37 °C. Obtained solution was diluted to 0.3 OD_{600} units using 1x LB medium and loaded in a 96 well plate (200 µL/well). The antibiotic or antibiotic-loaded NPs were added and the

OD600 was monitored every 5 minutes while incubating at 37 °C. When nanoparticles were used, they were prepared as described above at 800 µM. For studies including DNAse or RNAse 2 µL of 10 mg/mL RNAse or DNAse was added to each well.

4.4.5 Evaluation of antibiotic activity on porcine cornea

Corneas were taken from porcine eyes obtained from the local slaughterhouse and placed in a petridish. Kanamycin B- or neomycin B-loaded NPs were prepared at a concentration of 100 µM as described above. A rubber ring was placed around the cornea to prevent spillage and 100 µl of NP or free antibiotic solution was placed on top of the cornea. After 5 minutes incubation time, excess liquid was removed or the cornea was washed in a large excess of PBS (typical volume 10 ml) for the designated time. Subsequently, the corneas were placed on petrifilms (3M) prepared as recommended by the manufacturer. E. coli were grown at 37 °C overnight after which the amount of bacteria per ml LB medium was determined. Subsequently the suspension was diluted to obtain a final concentration of 10^4 E. coli/ml LB medium. On top of the corneas, on average 50 E. coli bacteria in 5 µl 1x LB medium were placed. For experiments with neomycinB 0.5 mg/ml RNAse was added to the medium. The petrifilms were incubated at 37 °C for 48 h after which pictures were taken. The number of colonies was determined in duplo by three persons with the pictures being blinded. Data are represented as mean +/- SD. Statistical analysis was performed using JMP® (version 10.0.0, SAS Institute Inc.). ANOVA analysis with Tukey-Kramer post-hoc test was used for statistical evaluation of the individual time-points and the negative cornea samples. Differences were considered to be significant at $p<0.05$.

4.4.6 Fluorescent labeling of aminoglycoside antibiotics

5-Carboxyfluorescein (5-FAM, 22.6 mg, 60 µmol) was dissolved in 250 µL of anhydrous DMF and activated by adding 1.2 eq of N-hydroxysuccinimide (NHS; 8.3 mg, 72 µmol) and dicyclohexylocarbodiimide (DCC; 14.96 mg,

72 µmol). The reaction mixture was gently shaken at room temperature for 3 h. The precipitate that was formed (dicyclohexylurea) was removed by centrifugation (5 min, 15k rpm) and crude supernatant containing 5-carboxyfluorescein succinimidyl ester was used without further purification. To ensure monomodification of the aminoglycosides, 1 eq (62.5 µL) of NHS-activated 5-FAM was subsequently added to 15 µmol of antibiotic in free base form (9.21 mg neomycin B; 7.24 mg kanamycin B) dissolved in 200µL of a water:dioxane mixture (2:1). After a reaction time of 2 h, 5-FAM-modified neomycin B (5-FAM-neomycin B) and kanamycin B (5-FAM-kanamycin B) were purified on Shimadzu VP series HPLC system with PDA detector using Zorbax SB-C18 3.5 µm column 75 x 4.6 mm (Agilent®). A linear gradient from 0 to 75% buffer B in 20 min was applied (A: 0.5% trifluoroacetic acid (TFA) and 5% CH_3CN in ultra-pure water, B: 100% CH_3CN). Purification was monitored at a wavelength of 440 nm. The purity and identity of the products was confirmed using RPC HPLC and ESI-MS (See Fig. 4.7 and Fig. 4.8). 5-FAM-neomycin B was obtained as TFA salt with 41% yield; ESI-MS (pos.) *m/z* 973.366 $[M+H]^+$ calc. 973.367 $[M+H]^+$. 5-FAM-kanamycin B was obtained as TFA salt with 35% yield; ESI-MS(pos.) *m/z* 842.308 $[M+H]^+$ calc. 842.309 $[M+H]^+$

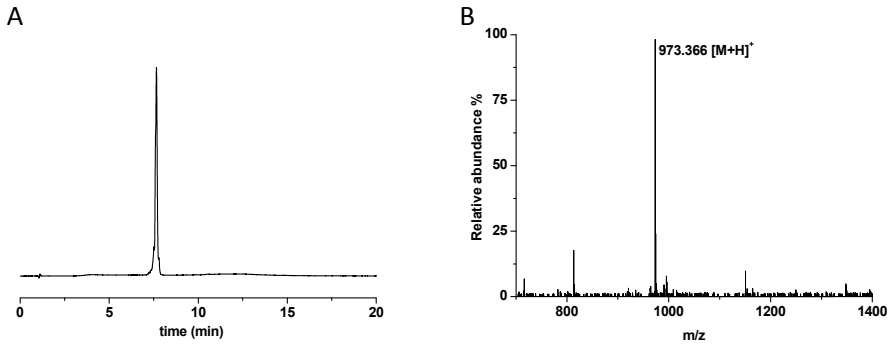

Figure 4.7. Characterization of 5-FAM-neomycin B conjugate. (A) HPLC chromatogram of purified product, (B) ESI-MS spectrum of purified product (calc. 973.367 [M+H]+, found m/z 973.366 [M+H]+).

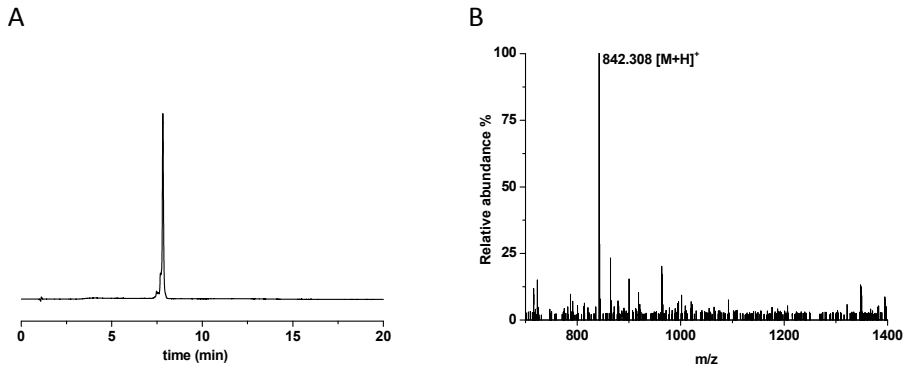

Figure 4.8. Characterization of 5-FAM-kanamycin B conjugate. (A) HPLC chromatogram of purified product, (B) ESI-MS spectrum of purified product (calc. 842.309 [M+H]+, found m/z 842.308 [M+H]+).

4.4.7 Nanoparticle (NP) imaging by transmission electron microscopy (TEM)

The amphiphiles were prepared at a concentration of 20 µM in 1x TAE buffer and thermally cycled (85°C, 30 min; -1°C/2 min until RT). Subsequently, 5 µl of NP solution was deposited on a glow-discharged carbon coated copper grid. Excess NP solution was blotted on a filter paper and the grid was washed once with ultrapure water and stained twice with a 2% uranyl acetate solution. Images were recorded using a CM12 transmission electron microscope (Phillips) at 120 kV. For size determination the diameter of 60 NPs was measured using ImageJ software (See Fig. 4.9).

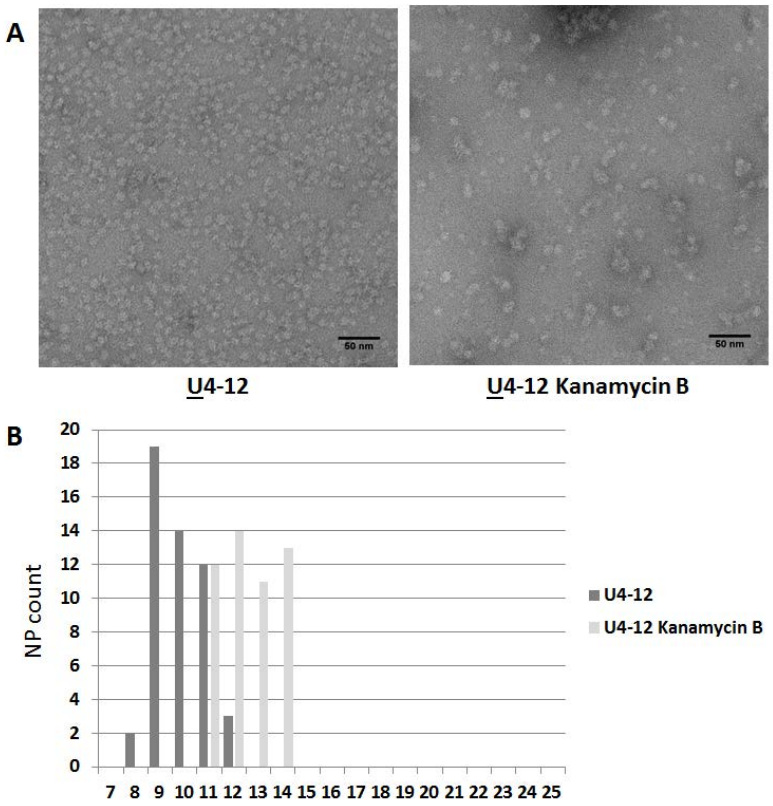

Figure 4.9. Transmission electron microscopy (TEM) images and size determination of bare and aptamer functionalized U4-12 micelles. (A) TEM images of bare U4-12 nanoparticles (left) and kanamycin B aptamer functionalized U4-12 carriers (right) and (B) size histogram of both NPs. Calculated average diameters are 10.0 ± 1.3 nm and 12.5 ± 1.4 nm for pristine and aptamer-functionalized NPs, respectively.

4.5 Acknowledgement

For the help with the TEM analysis of the pristine and aptamer functionalized NPs I would like to acknowledge the efforts of Agnieszka Gruszka. For the help with the statistical analysis of the bacterial growth on the cornea I would like to thank Sven Schnichels, Jose Hurst and Lisa Strudel.

4.6 References

[1] S. Shimmura, M. Ono, K. Shinozaki, I. Toda, E. Takamura, Y. Mashima, K. Tsubota, *Brit. J. Ophthalmol.* **1995**, *79*, 1007-1011.

[2] M. E. Johnson, P. J. Murphy, M. Boulton, *Graefes Arch. Clin. Exp.* **2006**, *244*, 109-112.

[3] M. E. Johnson, P. J. Murphy, M. Boulton, *Optometry Vision. Sci.* **2008**, *85*, 750-757.

[4] H. Y. Zhou, J. L. Hao, S. Wang, Y. Zheng, W. S. Zhang, *Int. J. Ophthalmol.* **2013**, *6*, 390-396.

[5] S. Y. Liu, L. Jones, F. X. Gu, *Macromol. Biosci.* **2012**, *12*, 608-620.

[6] C. Di Tommaso, A. Torriglia, P. Furrer, F. Behar-Cohen, R. Gurny, M. Moller, *Int. J. Pharm.* **2011**, *416*, 515-524.

[7] S. P. Ayalasomayajula, U. B. Kompella, *Eur. J. Pharmacol.* **2005**, *511*, 191-198.

[8] J. L. Cleland, E. T. Duenas, A. Park, A. Daugherty, J. Kahn, J. Kowalski, A. Cuthbertson, *J. Control. Release* **2001**, *72*, 13-24.

[9] I. Pepic, N. Jalsenjak, I. Jalsenjak, *Int. J. Pharm.* **2004**, *272*, 57-64.

[10] A. K. Gupta, S. Madan, D. K. Majumdar, A. Maitra, *Int. J. Pharm.* **2000**, *209*, 1-14.

[11] S. L. Law, K. J. Huang, C. H. Chiang, *J. Control. Release* **2000**, *63*, 135-140.

[12] N. Li, C. Y. Zhuang, M. Wang, X. Y. Sun, S. F. Nie, W. S. Pan, *Int. J. Pharm.* **2009**, *379*, 131-138.

[13] I. P. Kaur, D. Aggarwal, H. Singh, S. Kakkar, *Graefes Arch. Clin. Exp.* **2010**, *248*, 1467-1472.

[14] F. A. Aldaye, A. L. Palmer, H. F. Sleiman, *Science* **2008**, *321*, 1795-1799.

[15] J. W. de Vries, F. Zhang, A. Herrmann, *J. Control. Release* **2013**, *172*, 467-483.

[16] L. Gold, B. Polisky, O. Uhlenbeck, M. Yarus, *Annu. Rev. Biochem.* **1995**, *64*, 763-797.

[17] R. Stoltenburg, C. Reinemann, B. Strehlitz, *Biomol. Eng.* **2007**, *24*, 381-403.

[18] A. D. Ellington, J. W. Szostak, *Nature* **1990**, *346*, 818-822.

[19] C. Tuerk, L. Gold, *Science* **1990**, *249*, 505-510.

[20] K.-M. Song, M. Cho, H. Jo, K. Min, S. H. Jeon, T. Kim, M. S. Han, J. K. Ku, C. Ban, *Anal. Biochem.* **2011**, *415*, 175-181.

[21] L. Jiang, A. Majumdar, W. Hu, T. J. Jaishree, W. Xu, D. J. Patel, *Structure* **1999**, *7*, 817-827.

[22] T. N. Yusifov, A. R. Abduragimov, K. Narsinh, O. K. Gasymov, B. J. Glasgow, *Mol. Vis.* **2008**, *14*, 180-188.

[23] J. G. Souza, K. Dias, T. A. Pereira, D. S. Bernardi, R. F. Lopez, *J. Pharm. Pharmacol.* **2014**, *66*, 507-530.

[24] F. Lallemand, O. Felt-Baeyens, K. Besseghir, F. Behar-Cohen, R. Gurny, *Eur. J. Pharm. Biopharm.* **2003**, *56*, 307-318.

[25] M. Schultheiss, K. Januschowski, H. Ruschenburg, C. Schramm, S. Schnichels, P. Szurman, K. U. Bartz-Schmidt, M. S. Spitzer, *Graefes Arch. Clin. Exp.* **2013**, 1613-1619.